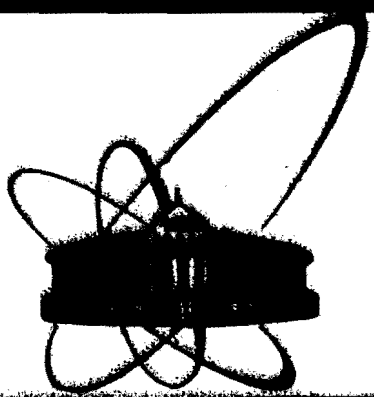

СООБЩЕНИЯ
ОБЪЕДИНЕННОГО
ИНСТИТУТА
ЯДЕРНЫХ
ИССЛЕДОВАНИЙ
ДУБНА

E17-87-724

E.Taranko, R.Taranko

CORRELATION EFFECTS IN EXTENDED HUBBARD MODEL. NUMERICAL RESULTS

1987

1. INTRODUCTION

A qualitative and quantitative understanding of electronic correlations in transition metals remains a challenging problem. The main theoretical problem is an appropriate treatment of the correlations between electrons. Angle-resolved experiments which have been performed recently for several of the 3d-band metals provide detailed information about electronic structure of these elements. Comparison of the experimental results with the existing band calculations reveals important discrepancies. Especially Ni is the case for which many-electron effects cannot be ignored [1]. For example, photoemission measurements indicate a total d-band width smaller by a factor of about 1.4 than in band structure calculations. Also, the value of the ferromagnetic exchange splitting at E_F of about 0.6-0.7 eV found in spin-polarized band calculations is roughly twice that required to fit angle-resolved and spin-polarized photoemission data. These and other discrepancies between one-electron theory and experiment indicate that the correlation between electrons must be included in a more transparent way. Up to the present, the Habbard Hamiltonian has been applied in most of the papers concerning the investigations of the many-body effects in solids, i.e., a large number of papers was devoted to investigations of model systems described by Hamiltonians with intraatomic integral present only. However, the intersite interactions may be important to the same degree (for detailed discussion see part I of this work [2]). For this reason we have investigated the influence of these additional interactions on the main specific feature of the many-body description, i.e., on the electron self-energy.

The paper is organized as follows. The Hamiltonian and the method of calculation of the self-energy as well as the approximations involved are discussed in Sec.II.Sec.III contains detailed numerical results of calculation of the electron self-energy for model fcc and scc tight-binding metals for various $\vec{k}$ vectors and values of intersite interactions. Also, a comparison with the so-called local approximation for self-energy is given.

2. THEORY

In part I of this paper[2] we have presented detailed theoretical investigations of the model Hamiltonian with intersite interactions included. Here, for the sake of completeness, we give only a short presentation of the obtained results (all notation is the same as in the previous paper[2]).

The Hamiltonian reads as

$$H = \sum_{ij\sigma} t_{ij} a^{+}_{i\sigma} a_{j\sigma} + \frac{U}{2} \sum_{i\sigma} n_{i\sigma} n_{i-\sigma} + \frac{1}{2} \sum_{ij\sigma} (1 - \delta_{ij})(U''_{ij} - I'_{ij}) n_{i\sigma} n_{j\sigma} + \tag{1}$$

$$+ \frac{1}{2} \sum_{ij\sigma} (1 - \delta_{ij}) U''_{ij} n_{i\sigma} n_{j-\sigma} + \frac{1}{2} \sum_{ij\sigma} (1 - \delta_{ij}) I''_{ij} a^{+}_{i\sigma} a^{+}_{i-\sigma} a_{j-\sigma} a_{j\sigma},$$

where U is the intraatomic Coulomb integral, U'', I', I'' are the interatomic Coulomb and exchange integrals. Usually, I' = = I'' in the case of real Wannier orbitals.

For a Fourier transform of the Green function defined as

$$G^{\sigma}_{ij}(t - t') \equiv \langle\langle a_{i\sigma}(t) ; a^{+}_{j\sigma}(t') \rangle\rangle \equiv -i\theta(t - t') \langle [a_{i\sigma}(t), a^{+}_{j\sigma}(t')]_{+} \rangle \tag{2}$$

we have obtained the Dyson equation

$$G^{\sigma}_{ij}(E) = G^{0\sigma}_{ij}(E) + \sum_{\ell n} G^{0\sigma}_{i\ell}(E) M^{\sigma}_{\ell n}(E) G^{\sigma}_{nj}(E), \tag{3}$$

where the Fourier transform of the "zeroth-order" Green function $G^{0\sigma}_{ij}(E)$ is as follows:

$$G^{0\sigma}(\vec{k}; E) = [E^{+} - \epsilon(\vec{k}) + \frac{1}{N} \sum_{\vec{q}} (U''(\vec{k} - \vec{q}) - I'(\vec{k} - \vec{q})) \langle n_{\vec{q}-\sigma} \rangle -$$

$$- \frac{1}{N} \sum_{\vec{q}} I''(\vec{k} + \vec{q}) \langle n_{\vec{q}-\sigma} \rangle - [U + U''(0)] \langle n_{-\sigma} \rangle - [U''(0) - I'(0)] \langle n_{\sigma} \rangle]^{-1}, \tag{4}$$

where

$$\epsilon(\vec{k}) = \frac{1}{N} \sum_{ij} t_{ij} e^{-i\vec{k} \cdot (\vec{R}_i - \vec{R}_j)} \tag{5}$$

$$\langle n_{\sigma} \rangle = \frac{1}{N} \sum_{\vec{q}} \langle n_{\vec{q}\sigma} \rangle .$$

The self-energy $M_{\sigma}(\vec{k};E)$ reads as

$$M_{\sigma}(\vec{k}; E) = \frac{1}{N^2} \sum_{\vec{p}\,\vec{q}} [\mathfrak{M}_{-\sigma\sigma-\sigma}(\vec{k}; E) f_1(\vec{k}, \vec{p}, \vec{q}) +$$

$$+ \mathfrak{M}_{-\sigma-\sigma\sigma}(\vec{k}; E) f_2(\vec{k}, \vec{p}, \vec{q}) + \mathfrak{M}_{\sigma\sigma\sigma}(\vec{k}; E) f_3(\vec{k}, \vec{p}, \vec{q})], \tag{6}$$

where

$$\mathfrak{M}_{\sigma_1\sigma_2\sigma_3}(\vec{k}; E) = \frac{1}{\pi^3} \int_{-\infty}^{+\infty} \iint \frac{d\omega_1 d\omega_2 d\omega_3}{E^{+} + \omega_1 - \omega_2 - \omega_3} \mathfrak{N}(\omega_1, \omega_2, \omega_3) \times \tag{7}$$

$$\times \operatorname{Jm} G^{\sigma_1}(\vec{p} + \vec{k}; \omega_1) \operatorname{Jm} G^{\sigma_2}(\vec{q} + \vec{p}; \omega_2) \cdot \operatorname{Jm} G^{\sigma_3}(\vec{q}; \omega_3),$$

$$f_1(\vec{k}, \vec{p}, \vec{q}) = U^2 + 2U U''(\vec{p}) + (U + U''(\vec{p})) I'(\vec{k} + \vec{p} + \vec{q}) + \tag{8a}$$

$$+ UU''(\vec{p}) + U''(\vec{p})^2,$$

$$f_2(\vec{k}, \vec{p}, \vec{q}) = I''(\vec{k} + \vec{p} + \vec{q}) [U + U''(\vec{k} - \vec{q}) + I''(\vec{k} + \vec{p} + \vec{q})], \tag{8b}$$

$$f_3(\vec{k}, \vec{p}, \vec{q}) = [I'(\vec{p}) - U''(\vec{p})] [U''(\vec{k} - \vec{q}) - I'(\vec{k} - \vec{q})] + \tag{8c}$$

$$+ [U''(\vec{p}) - I'(\vec{p})]^2,$$

$$\mathfrak{N}(\omega_1, \omega_2, \omega_3) = f(\omega_1) [1 - f(\omega_2)] [1 - f(\omega_3)] + \tag{8d}$$

$$+ [1 - f(\omega_1)] f(\omega_2) f(\omega_3),$$

and $f(\omega_1)$ is the Fermi distribution function, $U''(\vec{q})$, $I'(\vec{q})$, $I''(\vec{q})$ are the Fourier transforms of the intersite interactions.

III. SELF-ENERGY CALCULATIONS. NUMERICAL RESULTS AND DISCUSSION

Let us apply the results of the previous section to the calculations of the self-energy for a model electronic band structure. In general, formula (6) and

$$G^{\sigma}(\vec{k}; E) = [G^{0\sigma}(\vec{k}; E)^{-1} - M^{\sigma}(\vec{k}; E)]^{-1} \tag{9}$$

provide a self-consistent way for obtaining the self-energy $M^{\sigma}(\vec{k}; E)$ and Green function $G^{\sigma}(\vec{k}; E)$. However, because of rather tedious integration in 9-dimensional space (6-dimensio-

nal space for $\vec{k}$-integration and 3-dimensional space for energy integration) for every iteration step, we calculate the self-energy in the first iteration step only. Thus, we do not obtain self-consistent solutions of Eqs.(6) and (9), but for small values of U/W where W is the bandwidth, these results are quite reasonable, see also [3,4]. We take for $\mathrm{Im}G^{\sigma}(\vec{k}, E)$ as a first iteration step, the value

$$-\frac{1}{\pi}\,\mathrm{Im}G^{\sigma}(\vec{k}; E) = \delta(E - \epsilon(\vec{k})), \qquad (10)$$

where $\epsilon(\vec{k})$ is the energy dispersion for a model tight-binding energy band (in our case for fcc and scc crystal lattices). The spin index σ will be suppressed as we are dealing with the paramagnetic case.

Now formula (6) becomes

$$M(\vec{k}; E) = \frac{1}{N^2} \sum \frac{\mathfrak{N}(\vec{k}, \vec{p}, \vec{q})}{E^{+} + \epsilon(\vec{q}) - \epsilon(\vec{p} + \vec{q}) - \epsilon(\vec{k} + \vec{p})} [f_1(\vec{k}, \vec{p}, \vec{q}) + f_2(\vec{k}, \vec{p}, \vec{q}) + f_3(\vec{k}, \vec{p}, \vec{q})]. \qquad (11)$$

With the expression for the self-energy at hand, we can calculate the spectral density of states, the important characteristic of the electronic structure needed, for example, for interpretation of the photoemission spectra. For one-electron states the spectral density of states reduces to a set of delta functions peaked at the corresponding band energies, but in the presence of the electron correlations these peaks are shifted and broadened. These changes are essentially represented by the real and imaginary parts of the electron self-energy. Therefore, it would be particularly useful to investigate in detail the behaviour of the electron self-energy curves for a sufficiently broad class of parameters.

Let us discuss the method and class of parameters needed for calculation of the self-energy. The integrals were calculated by the Monte-Carlo method. For each energy and $\vec{k}$-vector from 500000 to 2×10^6 pairs of vectors $(\vec{p}, \vec{q})$ were randomly generated. In order to reduce a noise shown by the calculated curves, a very large number of randon points was needed especially for energies corresponding to the minimum of the self-energy. We first calculated, of course, the imaginary part of the self-energy and than obtained the real part by the Kramers-Kronig relation. Before we begin numerical calculations we must determine some parameters entering into the formulas for the self-energy (or, equivalently, the parameters of the Hamiltonian). The calculations were done for model fcc and scc crystal lattices with electron energy dispersion $\epsilon(\vec{k})$ calculated in tight-binding scheme for d-band with nearest-neighbour hopping integrals only. Although the Hamiltonian (1) describes the one-band model, we can try to use it for description, in an approximate manner, of the realistic many-band solids (see also [3,4]). If degenerate bands are considered, for simplicity, then in the calculated self-energy we must include the numerical factor 9 (for d-band metals) [3]. Of course, now the parameters U, U′, etc. are the average values taken over all pairs of the band indices. The bandwidth W and the band filling N_e were chosen to have reasonable values for modelling the d-band transition metals. We take W = 4.6 eV and the band filling N_e = 9.4 and 8.6 electrons per atom. These parameters correspond to nickel and cobalt, respectively. In order to obtain a better insight into the problem under consideration we have calculated the self-energy also for some other values of the parameters N_e. All calculations were done for the temperature 0°K and for the paramagnetic case. The next problem is the choice of the parameters describing the intersite Coulomb and exchange interactions. For fcc crystal lattice the Fourier transform of the interactions J_{ij} reads as (similarly for scc crystal lattice):

$$J(\vec{q}) = \frac{1}{N}\sum_{ij} e^{i\vec{q}\cdot(\vec{R}_i - \vec{R}_j)} J_{ij} = 4J^{(1)}\left[\cos\frac{aq_x}{2}\cos\frac{aq_y}{2} + \cos\frac{aq_y}{2}\cos\frac{aq_z}{2} + \cos\frac{aq_z}{2}\cos\frac{aq_x}{2}\right] + 2J^{(2)}\left[\cos(aq_x) + \cos(aq_y) + \cos(aq_z)\right] + \dots,$$

where $J^{(1)}$, $J^{(2)}$ are the first-neighbours and second-neighbours interactions, respectively, and a is a lattice constant. In our calculations we retain only the first term in this expression. Now we must determine the ratios $U/U''^{(1)}$, $U/I'^{(1)}$ (we have taken $I'_{ij} = I''_{ij}$). Note that the intersite integrals which are given by the matrix elements of the long-range Coulomb interaction, are defined with respect to the Wannier functions. Numerical values of these ratios are taken to be comparable with the ones used by Aisaka T. et al.[5,6] and Kaga E. et al.[7]. These authors found that including of the intersite interactions improves the consistency of the band narrowing and satellite binding energy as well as gives a correct $\vec{q}$-dependence of the effective exchange parameter in nickel. The numerical values for $(U/U''^{(1)}, U/I'^{(1)})$ we have

Fig.1. The imaginary and real parts of the self-energy (the left- (a) and right-hand side (b) parts of the Figure, respectively) for fcc *lattice.* E_F=0.95 eV, ($U/U''^{(1)}$, $U/I'^{(1)}$) =(10,20), $\vec{k}$ =(0,0,0).

used are (10,20), (10,50) and (20,100). In Figs. 1-10 we present results for imaginary and real parts of self-energy calculated for fcc crystal lattice; and in Figs.12-17, for scc crystal lattice. In all Figures the broken curves denote the result of local approximation for Hubbard Hamiltonian (see Appendix) and curves denoted by subscripts A, B and C correspond to the results obtained for the cases when all interactions are included - curve A, only on-site Coulomb interaction is present - (Hubbard model) - curve B and on-site Coulomb and intersite Coulomb interactions are taken into account - curve C, respectively. In all Figures the left part represents the imaginary part of the self-energy and the right part - the real part of the self-energy. If in any Figure the curve denoted by letter C is absent, it means that there is no difference between curves A and C.

In Figs. 1-3, 4-6 and 7-9 the self-energy curves are calculated for the parameters ($U/U''^{(1)}$, $U/I'^{(1)}$) equal to (10,20) (10,50) and (20,100), respectively. In order to obtain a better insight into the problem we have calculated the self-energy for different $\vec{k}$-vectors in Brillouin zone, namely for $\vec{k}$ = (0,0,0) — Γ, $\vec{k}$ = (1/2, 1/2, 1/2) $2\pi/a$ — L, and for $\vec{k}$ = =(1,0,0)$2\pi/a$ — X. The energy band for fcc is located in the limits (-3.45 eV, 1.15 eV) and E_F = 0.95 eV. This value of Fermi energy corresponds approximately to the band-filling equal to 8,6 electrons/atom (in degenerate d-bands model) and roughly corresponds to the case of Co and may be representative, to some extent in our model calculations, of transition metals Ni, Co, Fe for which this parameter takes the values 9.4, 8.4 and 7.3 electrons/atom, respectively. Additionally, we present the imaginary part of the self-energy calculated for fcc lattice for E_F = 0.25 eV (50% of the total band filling) and for ($U/U''^{(1)}$, $U/I'^{(1)}$) equal to (10,20), Fig.11. In the case of scc lattice we placed the Fermi energy in the middle of the band and took for the parameters ($U/U''^{(1)}$, $U/I'^{(1)}$) values (10,50) Figs.12-14 and (20,100), Figs.15-17.

Let us discuss the case of fcc lattice. First of all, when looking at Figs.1-9, it is seen at once that there is a very clear dependence of the electron self-energy on $\vec{k}$-vector independent of the value of the electron-electron interactions.

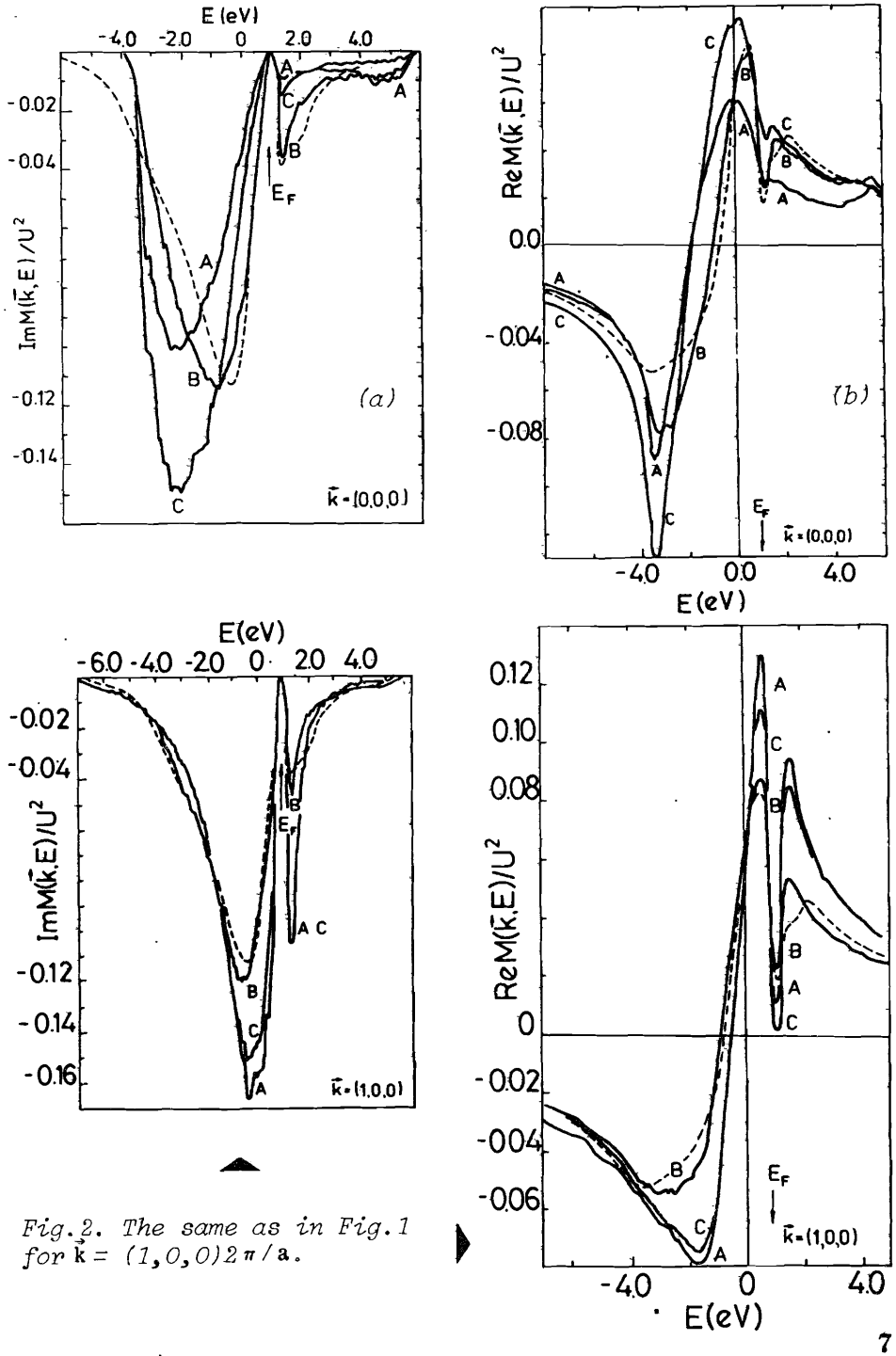

Fig.2. The same as in Fig.1 for $\vec{k}$ = $(1,0,0)2\pi/a$.

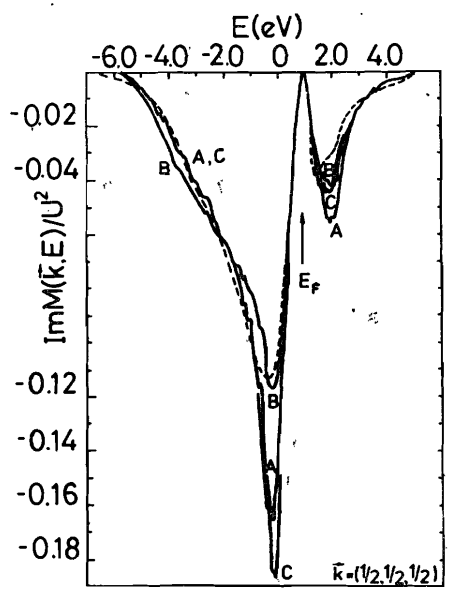

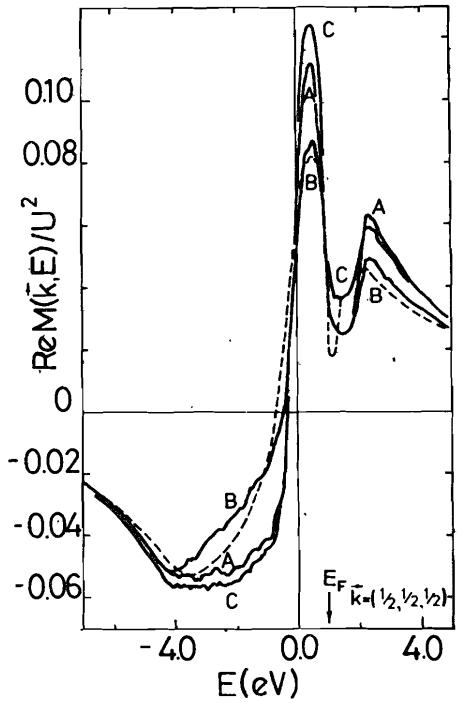

Fig. 3. The same as in Fig. 1 for $\vec{k} = (1/2, 1/2, 1/2)\,2\pi/a$.

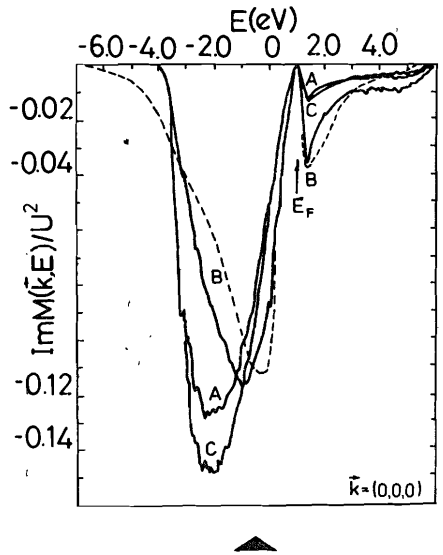

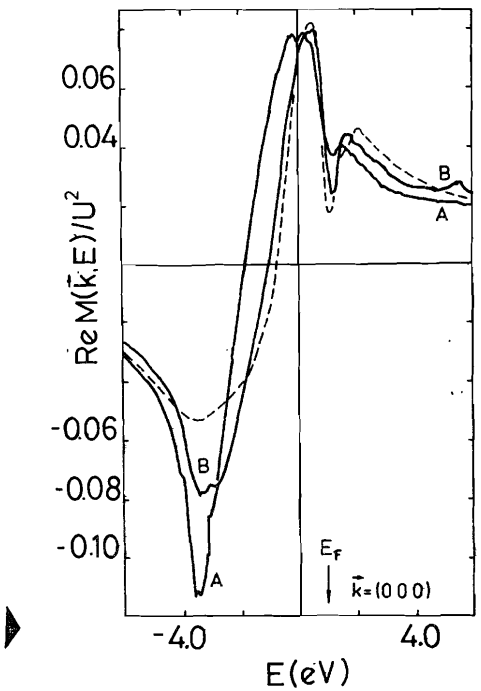

Fig. 4. The same as in Fig. 1 for $(U/U''^{(1)},\ U/I'^{(1)}) = (10, 50)$.

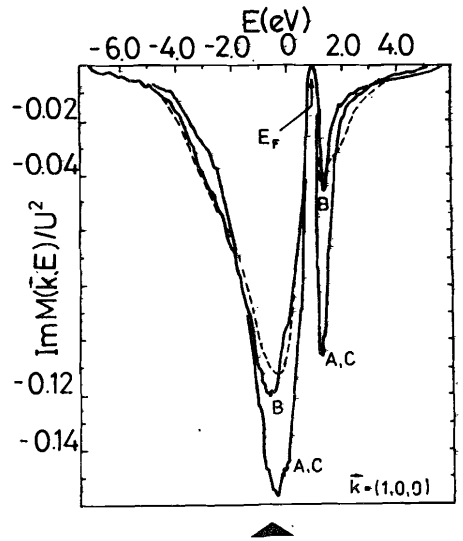

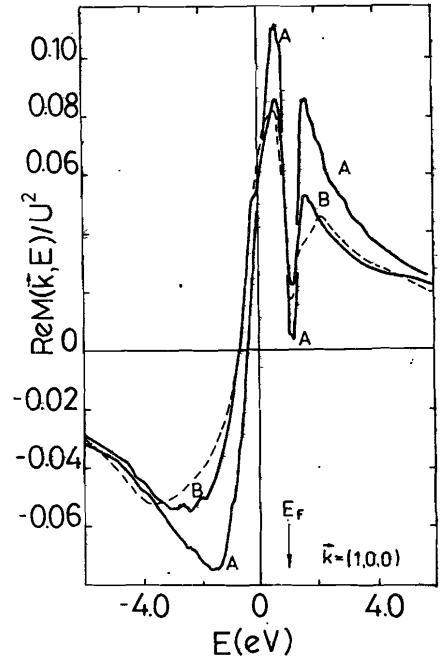

Fig. 5. The same as in Fig. 4 for $\vec{k} = (1, 0, 0)\,2\pi/a$.

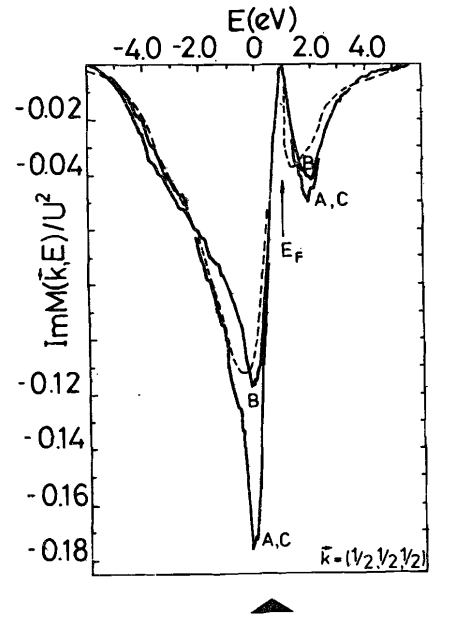

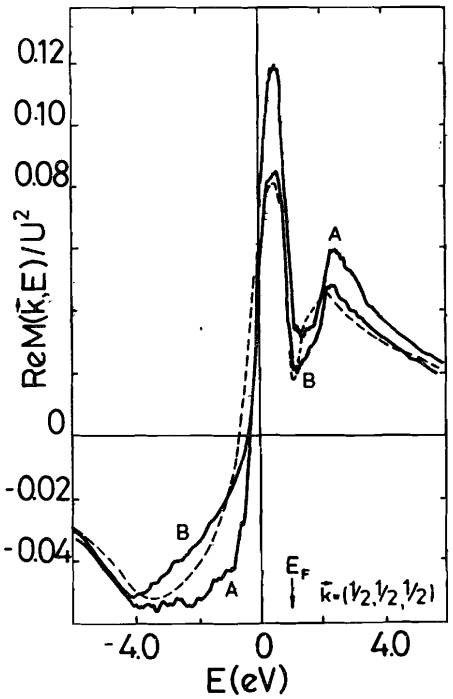

Fig. 6. The same as in Fig. 4 for $\vec{k} = (1/2, 1/2, 1/2)\,2\pi/a$.

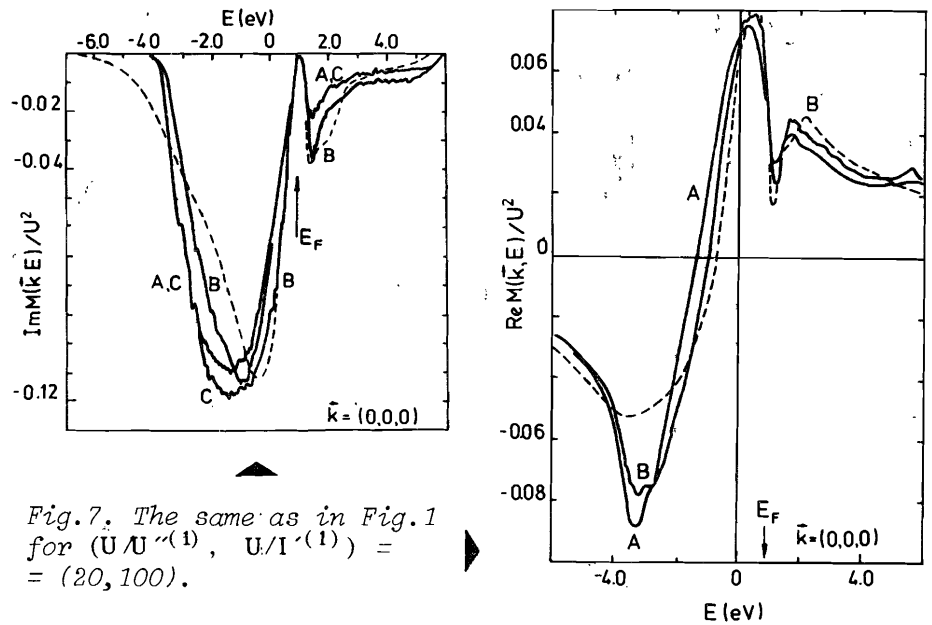

Fig.7. The same as in Fig.1 for $(U/U'^{(1)},\ U/I'^{(1)}) = (20, 100)$.

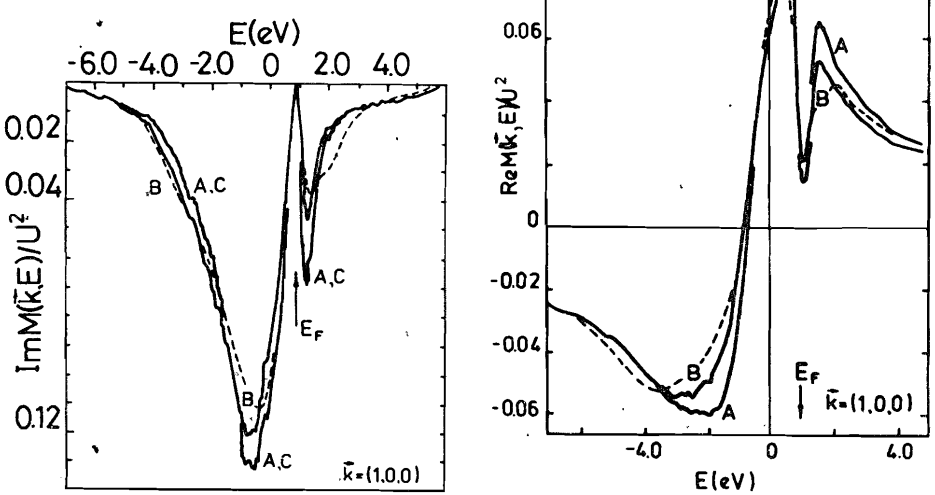

Fig.8. The same as in Fig.7 for $\vec{k} = (1,0,0)2\pi/a$.

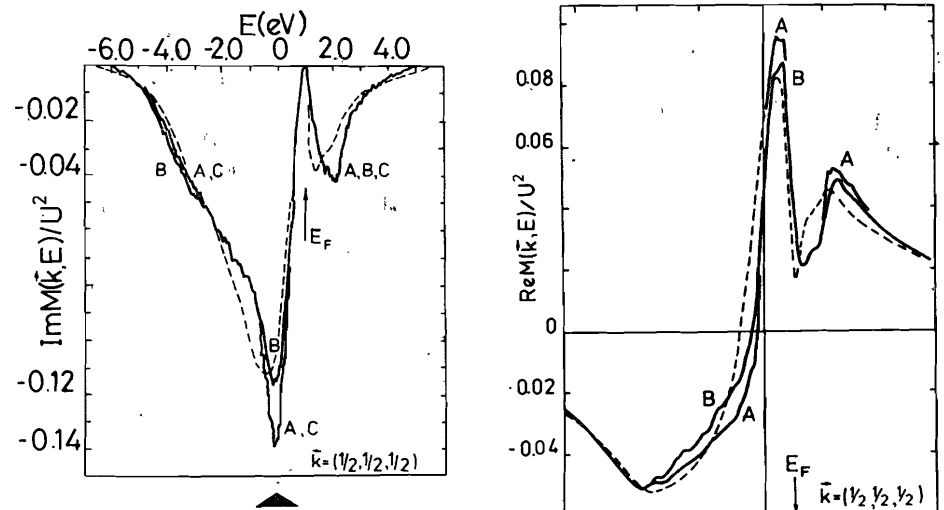

Fig.9. The same as in Fig.7 for $\vec{k} = (1/2, 1/2, 1/2)2\pi/a$.

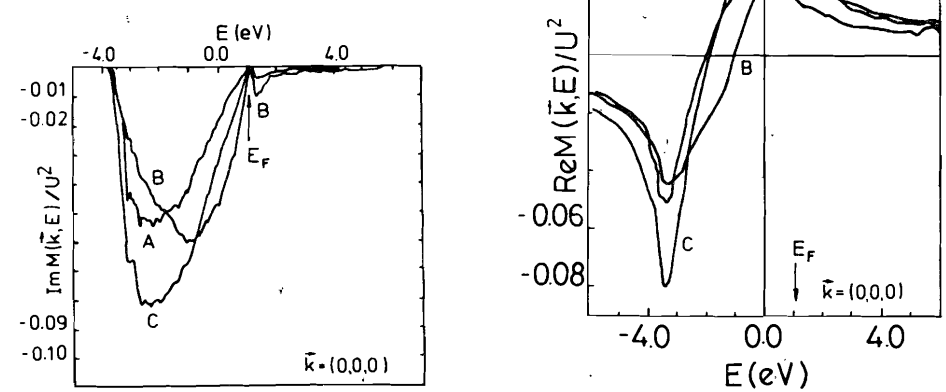

Fig.10. The same as in Fig.1 for $E_F = 1.07$ *eV.*

Fig. 11. The imaginary part of the self-energy for fcc *lattice,* $E_F = 0.25$ *eV,* $\vec{k} = (0,0,0)$, $(U/U''^{(1)}, U/I'^{(1)}) = (10,20)$.

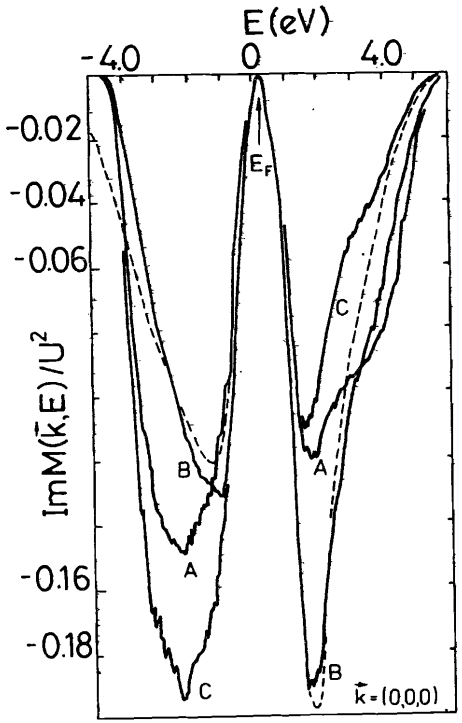

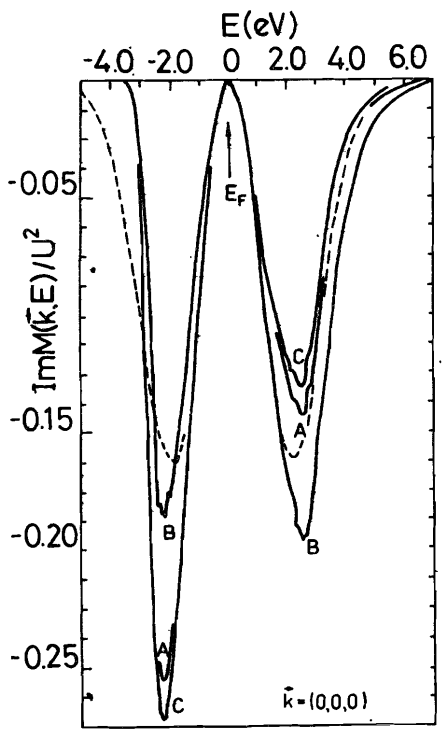

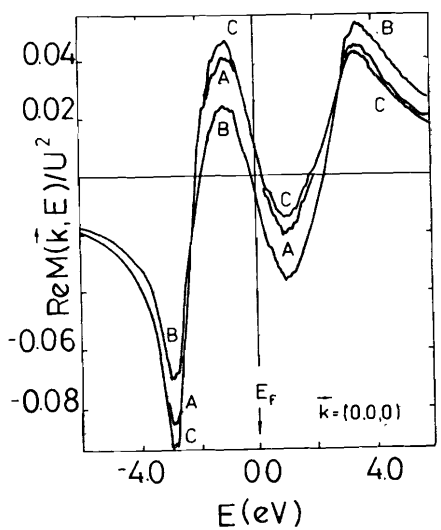

Fig. 12. The same as in Fig. 1 for scc *lattice,* $E_F = 0.0$ *eV and* $(U/U''^{(1)}, U/I'^{(1)}) = (10,50)$.

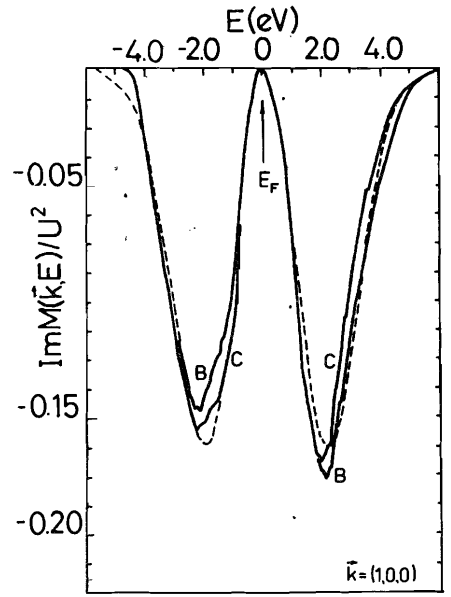

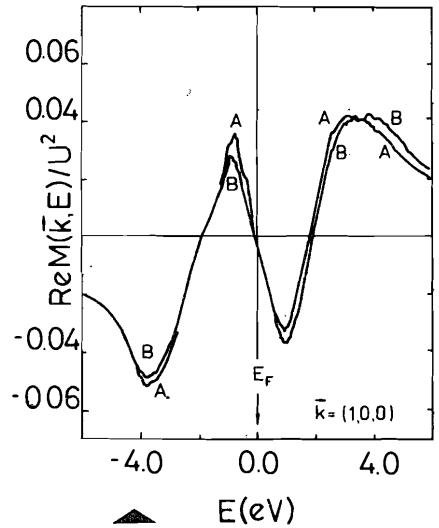

Fig. 13. The same as in Fig. 12 for $\vec{k} = (1,0,0)\pi/a$.

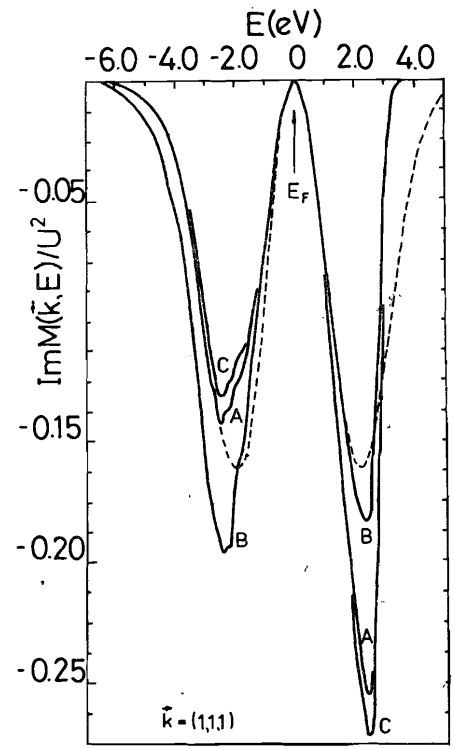

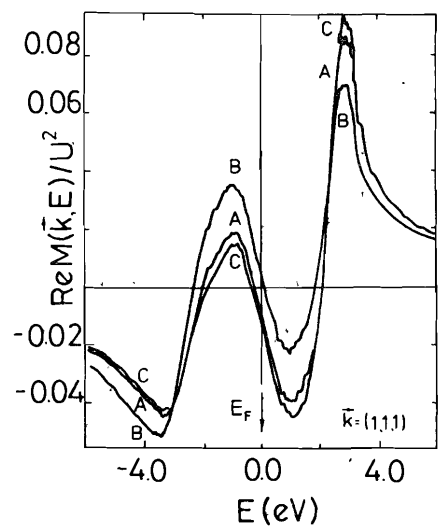

Fig. 14. The same as in Fig. 12 for $\vec{k} = (1,1,1)\pi/a$.

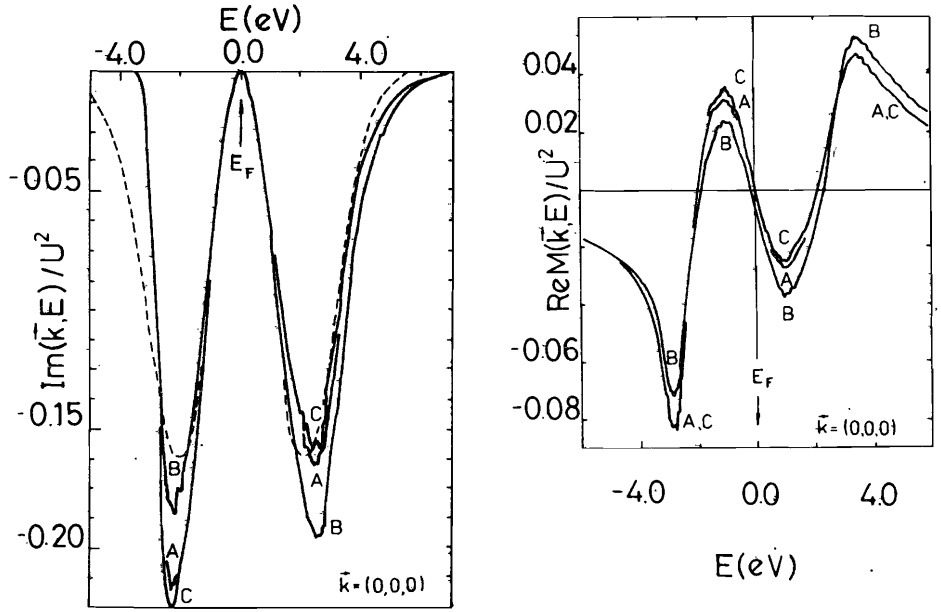

Fig. 15. The same as in Fig. 12 for $(U/U''^{(1)}, U/I'^{(1)}) = (20, 100)$.

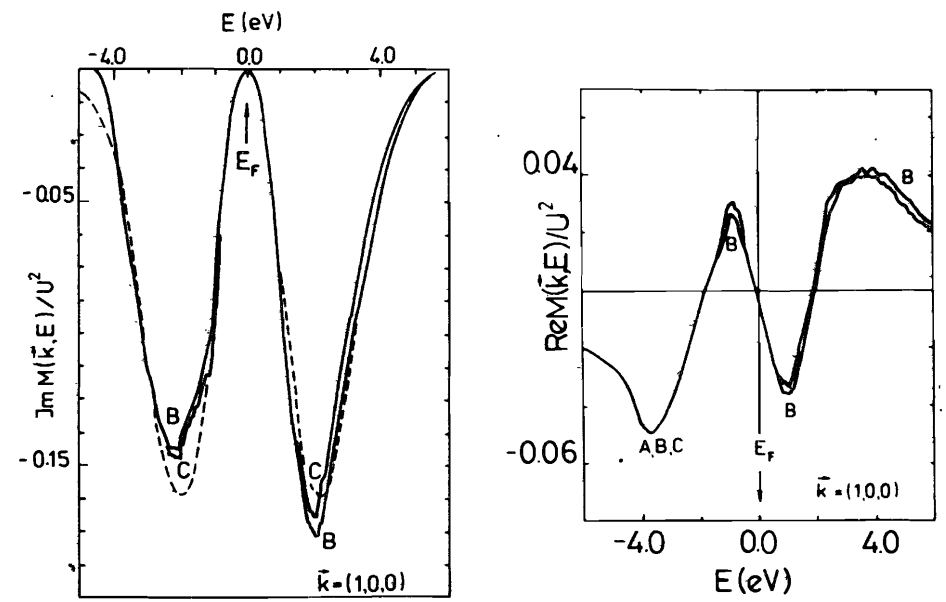

Fig. 16. The same as in Fig. 15 for $\vec{k} = (1,0,0)\pi/a$.

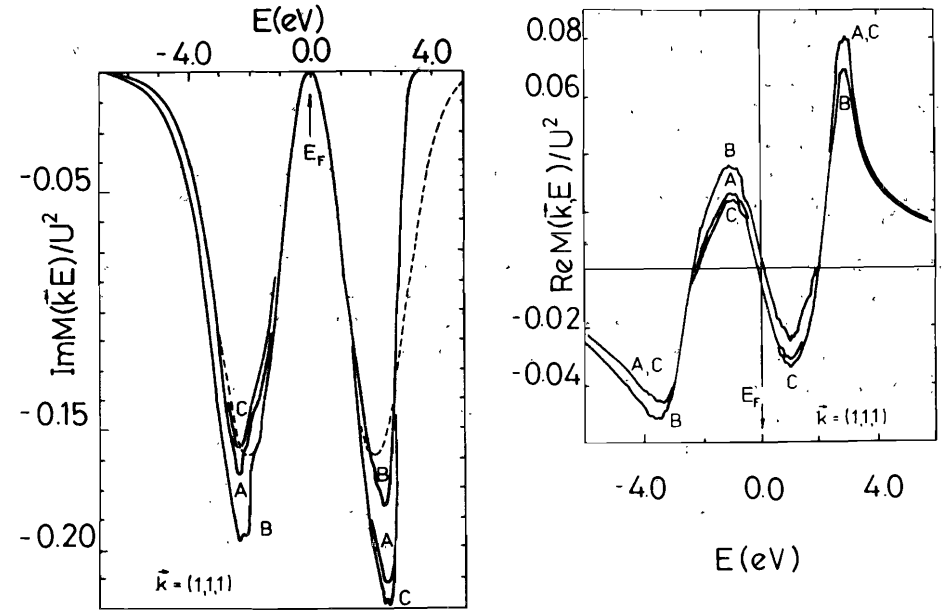

Fig. 17. The same as in Fig. 15 for $\vec{k} = (1,1,1)\pi/a$.

The imaginary part of the self-energy for $\vec{k} = (0,0,0)$ has a nonvanishing value in the energy interval from -4.0 eV to 6.0 eV and has no any tails for energies below as well as above the Fermi energy. On the other hand, it has a rather broad main minimum extended to -0.15. As we are going with $\vec{k}$-vector from Γ point of the Brillouin zone to more distant $\vec{k}$-points, the imaginary part of the self-energy has long nonvanishing tails and both the minima are larger and sharp. Especially sharp main minimum (for energies below the Fermi energy) has the imaginary part of the self-energy for the point $(1/2, 1/2, 1/2)2\pi/a$, whereas for the point $(1,0,0)2\pi/a$ minimum for energies above Fermi energy has a very small value. This general trends are independent of the value of the electron-electron interaction. For the cases outlined above, also the real part of the self-energy changes from the shape with relatively sharp minima below and in the neighbourhood of E_F for Γ - point to the shape with a very broad minimum below E_F and relatively sharp structure (two maxima and one minimum) near the Fermi energy. The local approximation, which is very often used in literature for a Hubbard Hamiltonian, is a rather good approximation for $\vec{k}$-vectors lying at a distance from Γ point.

For Γ point the discrepancies between the exact calculation and those done in the local approximation reach about 25% in the region of a broad minimum. The imaginary part of the self-energy calculated in the local approximation has a tail spreading outside the limits obtained from the exact calculations (for Γ point, only).

As for a comparison of the numerical values for the self-energy, we can say that biginning from the parameters $(U/U'^{(1)}, U/I'^{(1)})$ equal to (20,100) the differences between those calculated for the Hubbard Hamiltonian (but for $\vec{k}$-dependent self-energy) and for the Hamiltonian with inter-site electron-electron interactions included, are relatively small for $\vec{k}=(0,0,0)$ (excluding the energy region corresponding to minima or maxima of imaginary or real parts of self-energy) and are negligible for $\vec{k}$ points lying outside the middle of the Brillouin zone. In Fig.10 we present the imaginary and real parts of self-energy calculated for $E_F = 1.07$ eV for fcc lattice. This Fermi energy corresponds to the band filling equal to 94% (for degenerate d-band Hamiltonian this corresponds to 9,4 electrons/atom). All the conclusions we have made for the case of the Fermi energy equal to 0.95 eV are now justified too. The only difference is smaller numerical values for the calculated self-energy curves. In order to better show the influence of the intersite electron-electron interactions on the self-energy, we present in Fig.11 the imaginary part of the self-energy calculated for a band filling of the fcc energy band equal to 50% (for $\vec{k} = (0,0,0)$). In this case the top of the density of states is located far away from E_F and the imaginary part of the self-energy for Hubbard Hamiltonian (also, in the local approximation) is strongly unsymmetric curve. Surprisingly, after including the electron-electron intersite interactions we have a quite different situation. Now the location of the minima is interchanged and we obtain the minimum for energies below E_F. Such a situation leads to quite different pictures for the spectral density of states. Now we have broad peaks of the spectral density of states for energies below E_F and not for energies greated than E_F.

In Figs.12-14 and 15-17 we present the self-energy for scc crystal lattice for $(U/U'^{(1)}, U/I'^{(1)})$ equal to (10,50) and (20,100), respectively, for different $\vec{k}$-vectors. The Fermi energy is located in the middle of the band. The band is located, in the energy scale from -2.3 eV to 2.3 eV. In comparison with the previous results for fcc crystal lattice, now for $(U/U'^{(1)}, U/I'^{(1)})$ equal to (20,100) influence of the electron-electron intersite interactions is quite noticeable. Comparing these results (and these for $(U/U'^{(1)}, U/I'^{(1)})$ equal to (10,50)) with those for the Hubbard Hamiltonian, we can observe quite a different behaviour of the calculated curves for the imaginary parts of self-energy for different points of the Brillouin zone. Generally, we have strong minimum for energy below E_F for $\vec{k} = (0,0,0)$ comparing with the imaginary part of the self-energy calculated for the Hubbard Hamiltonian. On the other hand, for energies greater than E_F a greater minimum is obtained for Hubbard Hamiltonian. This situation is interchanged when we are going to $\vec{k}$-vector $(1,1,1)\pi/a$. For $\vec{k} = (1,0,0)\pi/a$ the self-energy ($\vec{k}$- dependent) calculated for the Hubbard Hamiltonian and for the extended Hubbard Hamiltonian is comparable.

In conclusion, we have calculated $\vec{k}$-dependent electron self-energy for the extended Hubbard Hamiltonian for small values of U/W for fcc and scc crystal model band structures for the parameters representing, to some extent, the real transition metals. The obtained results indicate a relatively great influence of the intersite electron-electron interaction on the electron self-energy. The changes in the behaviour of these self-energy curves depending on the values of $(U/U'^{(1)}, U/I'^{(1)})$ and $\vec{k}$-vector may lead to relatively great changes in the spectral density of states which is very important, especially in various photoemission studies.

APPENDIX

Here we give connection between the general expression for self-energy given in Eq.(6) and the so-called local approximation introduced and discussed by Treglia et al.[3] for the self-energy calculated in second-order perturbation theory in U/W for a degenerate Hubbard Hamiltonian. Namely, Eq.(6) can be rewritten in the form (paramagnetic case)

$$M(\vec{k};E) = \frac{1}{N^2}\sum_{\vec{R}} e^{i\vec{k}\cdot\vec{R}} \iiint_{-\infty}^{+\infty} \frac{d\omega_1 d\omega_2 d\omega_3}{E^+ + \omega_1 - \omega_2 - \omega_3} \Pi(\omega_1, \omega_2, \omega_3) \times$$

$$\times \left(-\frac{1}{\pi}\right)^3 \sum_{\vec{k}_2,\vec{k}_3,\vec{k}_4} e^{i\vec{k}_2\cdot\vec{R}} \mathrm{Im}\, G(\vec{k}_2;\omega_1)\, e^{i\vec{k}_3\cdot\vec{R}}\, \mathrm{Im}\, G(k_3;\omega_2) \times \qquad (A.1)$$

$$\times e^{i\vec{k}_4\cdot\vec{R}}\,\mathrm{Jm}\,G(\vec{k}_4,\omega_3)\times[f_1(\vec{k}_4-\vec{k}_2+\vec{k}_3,\ \vec{k}_2-\vec{k}_3,\ \vec{k}_3)+$$

$$+ f_2(\vec{k}_4-\vec{k}_2+\vec{k}_3,\ \vec{k}_2-\vec{k}_3,\ \vec{k}_3)+f_3(\vec{k}_4-\vec{k}_2+\vec{k}_3,\ \vec{k}_2-\vec{k}_3,\ \vec{k}_3)],$$

where $\mathfrak{N}(\omega_1,\omega_2,\omega_3)$, $f_i(\vec{k},\vec{p},\vec{q})$, $i=1,2,3$ are given in Eqs.(8D, 8A, 8B, 8C), respectively, and $\vec{R}$ denotes atomic positions in the crystal. When we consider the Hubbard Hamiltonian ($U''=I'=I''=0$), then from Eq.(A.1) the result of Treglia et al.[3] is obtained

$$M(\vec{k};E)=U^2\sum_{\vec{R}}e^{i\vec{k}\cdot\vec{R}}\int_{-\infty}^{+\infty}\!\!\int\!\!\int\frac{d\omega_1 d\omega_2 d\omega_3}{E^+ +\omega_1-\omega_2-\omega_3}\,\mathfrak{N}(\omega_1,\omega_2,\omega_3)\times$$

$$\times D(\vec{R};\omega_1)\,D(\vec{R};\omega_2)\,D(\vec{R};\omega_3), \qquad (A.2)$$

where

$$D(\vec{R};\omega)=\frac{1}{N}\sum\left(-\frac{1}{\pi}\right)\mathrm{Jm}\,G(\vec{k};\omega)\,e^{i\vec{k}\cdot\vec{R}}. \qquad (A.3)$$

If we retain only the first term in (A.2)- local approximation - then for $T=0^\circ K$ we have

$$M(\vec{k};E)\to M(E)=U^2\Big(\int_a^{E_F}d\omega_1\int_{E_F}^{b}d\omega_2\int_{E_F}^{b}d\omega_3+$$

$$+\int_{E_F}^{b}d\omega_1\int_a^{E_F}d\omega_2\int_a^{E_F}d\omega_3\Big)\frac{D(\omega_1)D(\omega_2)D(\omega_3)}{E^+ +\omega_1-\omega_2-\omega_3}. \qquad (A.4)$$

From Eq.(A.1) it is evident that in the case of including in the Hamiltonian of the intersite electron interactions, it is impossible to obtain expression like (A.2) with factorized lattice Green functions. For that reason, in the case of Hamiltonians with intersite interactions included, the local approximation does not give any facility in the calculation of the self-energy.

REFERENCES

1. Eastman D.E. et al. - J.Appl.Phys., 1979, 50, p.7423.
2. Taranko R., Taranko E. JINR Preprint E17-87-282, Dubna, 1987.

3. Treglia G., Ducastelle F., Spanjaard D. - J.Physique, 1980, 41, p.281.
4. Treglia G., Ducastelle F., Spanjaard D. - J.Physique, 1982, 43, p.341.
5. Aisaka T., Kato T., Haga E. - Phys.Rev.B, 1983, 28, p.1113.
6. Aisaka T., Kato T., Haga E. - J.Phys.F, 1984, 14, p.2537.
7. Haga E., Kato T., Aisaka T. - Progr.Theor.Phys., 1978, 59, p.697.

Submitted by Publishing Department
on October 2, 1987.

SUBJECT CATEGORIES OF THE JINR PUBLICATIONS

Index	Subject
1.	High energy experimental physics
2.	High energy theoretical physics
3.	Low energy experimental physics
4.	Low energy theoretical physics
5.	Mathematics
6.	Nuclear spectroscopy and radiochemistry
7.	Heavy ion physics
8.	Cryogenics
9.	Accelerators
10.	Automatization of data processing
11.	Computing mathematics and technique
12.	Chemistry
13.	Experimental techniques and methods
14.	Solid state physics. Liquids
15.	Experimental physics of nuclear reactions at low energies
16.	Health physics. Shieldings
17.	Theory of condenced matter
18.	Applied researches
19.	Biophysics

Таранко Э., Таранко Р. E17-87-724

Корреляционные эффекты в расширенной модели Хаббарда. Численные расчеты

Модель Хаббарда обобщается на случай включения дальнодействующего кулоновского взаимодействия между электронами, находящимися на разных узлах кристаллической решетки. В рамках формализма двухвременных функций Грина проведены численные расчеты действительной и мнимой части массового оператора для различных параметров, описывающих модельные металлы. Показано, что включение междуузельных электронных взаимодействий ведет к значительным изменениям собственной энергии электронов.

Работа выполнена в Лаборатории теоретической физики ОИЯИ.

Сообщение Объединенного института ядерных исследований. Дубна 1987

Taranko E., Taranko R. E17-87-724

Correlation Effects in Extended Hubbard Model. Numerical Results

The Hubbard Hamiltonian is extended to include long-range Coulomb interactions between electrons on different atomic sites. Electron self-energy for various parameters describing the model tight-binding fcc and scc metals is calculated. It is shown that inclusion of the intersite electron interactions leads to considerable changes of the electron self-energy.

The investigation has been performed at the Laboratory of Theoretical Physics, JINR.

Communication of the Joint Institute for Nuclear Research. Dubna 1987